

Enhancement of octupole strength in near spherical nuclei

L. M. Robledo¹ ^a

Dep. Física Teórica, Facultad de Ciencias, Universidad Autónoma de Madrid, E-28049 Madrid, Spain

Received: date / Revised version: date

Abstract. The validity of the rotational formula used to compute E1 and E3 transition strengths in even-even nuclei is analyzed within the Generator Coordinate Method framework based on mean field wave functions. It turns out that those nuclei with spherical or near spherical shapes the E1 and E3 strengths computed with this formula are strongly underestimated and a sound evaluation of them requires angular momentum projected wave functions. Results for several isotopic chains with proton number equal or near magic numbers are analyzed and compared with experimental data. The use of angular momentum projected wave functions greatly improves the agreement with the scarce experimental data.

PACS. 21.60.-n Nuclear structure models and methods – 21.60.Jz Nuclear Density Functional Theory and extensions

1 Introduction

The study of octupole correlations is of fundamental importance to understand the properties of low lying collective states of negative parity in atomic nuclei [1]. Octupole deformation can be static, when the nuclear wave function breaks the symmetry under spatial reflection leading to a non-zero octupole moment or dynamic when it preserves the symmetry but quantum fluctuations involving octupole shapes are relevant [2]. The observables of interest associated with octupole correlations include the excitation energy of collective negative parity states and the electromagnetic transition strengths of E1 and E3 type connecting them to the ground state. Although the presence of permanent octupole deformation is scarce in even-even nuclei dynamical octupole correlations are pervasive over all the periodic table. In spherical nuclei octupole vibrational excited states are also common and they are characterized by very collective E3 transition strengths.

The study of the properties of collective negative parity states in even-even nuclei has been recently addressed using several variants of the Gogny force in the framework of the Generator Coordinate Method (GCM) [3] with the axial octupole moment as generating coordinate. Results for the excitation energy of the collective negative parity state as well as the E1 and E3 transition strengths to the ground state were obtained. The comparison with experimental data revealed a systematic over-estimation of the excitation energy. Concerning the transition strengths, there was a systematic behavior indicating a much better reproduction of the strength in well deformed nuclei.

In addition to this study, the impact of static and dynamic octupole correlation on the binding energies of the

ground state of even-even nuclei has been considered in [4]. It was shown there that all even-even nuclei show octupole dynamic correlations with energy gains in the range in between one and two MeV but with a smooth behavior as a function of proton or neutron number.

A subsequent analysis of the E3 transition strengths obtained with mean field states, revealed [5] that the rotational formula used to compute them is not valid in spherical or weakly quadrupole deformed systems. A careful analysis of the general structure of the wave function near sphericity revealed that, in that case, the transition strength had to be up to a factor 7 ($2I + 1$ with $I = 3$) larger than the value provided by the rotational formula.

2 Theoretical framework

As it is customary in nuclear structure, the theoretical framework is based on the mean field Hartree-Fock-Bogoliubov (HFB) method [6]. A set of HFB intrinsic wave functions is generated using the axially symmetric octupole moment Q_{30} as a constraint and considering a mesh of octupole moments adapted to the problem at hand. The wave functions generated this way break reflection symmetry. In many cases, they also break rotational invariance and particle number and therefore the wave functions belong to the category of intrinsic wave functions, that is the symmetry quantum numbers have to be restored in order to compute quantities in the laboratory frame. For the energy density functional (EDF) we have used the Gogny EDF [7] with the D1S parametrization [8]. Most of the quantities discussed in the present paper have also been obtained with the D1M [9] and D1N [10]. The comparison with the D1S results reveal many similitudes

^a luis.robledo@uam.es

and therefore only the latter have been considered here. A highly optimized computer code using second order gradient information [11] is used in the calculations. In the computer code, the quasiparticle operators are expanded in a harmonic oscillator basis containing a number of major shells that depends on the mass number of the nucleus to be treated and large enough as to guarantee the convergence of excitation energies and transition strengths - see [3] for details. The set of HFB wave functions $|\varphi(Q_3)\rangle$ is subsequently used in several beyond mean field schemes discussed below.

2.1 Parity Projection

The first step beyond the mean field is to recover some of the broken symmetries of the intrinsic states. To restore reflection symmetry (associated to the parity quantum number) we use the parity projection operator $P_\pi = 1 + \pi \hat{H}$ which is a linear combination of the symmetry operations: identity and parity \hat{H} . The relative amplitudes of the linear combination determine the quantum number $\pi = \pm 1$ of the restored symmetry. Applying the projector to the intrinsic states $|\varphi(Q_3)\rangle$ we obtain states with good parity π that can be used to compute observable quantities like the energy. As there are two possible values of the parity, there are also two energies E_π . In the restricted variation after projection (RVAP) scheme [6] the parity projected energies E_π are computed for each member of the set of intrinsic states $|\varphi(Q_3)\rangle$ and the two minima determine the optimal intrinsic states for each parity. In even-even nuclei where the positive parity state is always more bound than the negative parity one, the lowest positive parity state is associated to the ground state whereas the negative parity one is associated to the lowest lying negative parity state. This negative parity state that can be, depending on the deformation of the nucleus, the band head of a negative parity rotational band in the case of a quadrupole deformed nucleus or a 3^- vibrational state in case of a weakly or spherical nucleus. In order to compute transition strengths between the negative parity and the ground state the rotational formula is assumed. For instance, assuming axially symmetric states

$$B(E3, 3^- \rightarrow 0^+) = \frac{e^2}{4\pi} \langle \Psi_- | \hat{Q}_{30} \frac{1+t_z}{2} | \Psi_+ \rangle^2. \quad (1)$$

with $\hat{Q}_{30} = z(z^2 - \frac{3}{2}(x^2 + y^2))$ the $K = 0$ component of the octupole moment. The rotational formula is based on the rotational assumption and is used to connect intrinsic quantities with quantities in the lab system like transition strengths. This scheme is used in [3] to compute E1 and E3 transition strengths of essentially all relevant even-even nuclei. A comparison with the E3 experimental compilation of Ref [12] reveals that the theoretical predictions agree much better with experiment when the nucleus is well quadrupole deformed.

2.2 Generator coordinate method

The generator coordinate method (GCM) considers linear combinations of a set of relevant mean field states (like the set $|\varphi(Q_3)\rangle$ mentioned above) to create correlated wave functions

$$|\Psi_\sigma\rangle = \int dQ_3 f_\sigma(Q_3) |\varphi(Q_3)\rangle \quad (2)$$

labeled by σ . Usually, instead of continuum variables Q_3 a discrete set $\{Q_{3,i}, i = 1, \dots, N\}$ is considered; the integral is then replaced by a sum. The amplitudes $f_\sigma(Q_3)$ are determined by the variational principle on the energy what leads to the Hill-Wheeler equation

$$\int dQ'_3 \langle \varphi(Q_3) | (\hat{H} - E_\sigma) | \varphi(Q'_3) \rangle f_\sigma(Q'_3) = 0 \quad (3)$$

requiring the norm

$$\mathcal{N}(Q_3, Q'_3) = \langle \varphi(Q_3) | \varphi(Q'_3) \rangle$$

and Hamiltonian

$$\mathcal{H}(Q_3, Q'_3) = \langle \varphi(Q_3) | \hat{H} | \varphi(Q'_3) \rangle$$

overlaps. These quantities are computed with the generalized Wick theorem and the pfaffian formula [13, 14, 15, 16]. The evaluation of the hamiltonian overlap for density dependent interactions is still subject to some conceptual difficulties - see [17] for a discussion involving the octupole degree of freedom. Once the $f_\sigma(Q_3)$ amplitudes are obtained, the transition strength is computed with the formula of Eq 1 but using for the $|\Psi_+\rangle$ and $|\Psi_-\rangle$ wave functions the GCM states obtained for the ground and first excited state, respectively. As in the RVAP parity projection calculation discussed above, the results obtained for a compilation of even-even nuclei [3] and the comparison with experimental data revealed a pattern associated with the quadrupole deformation of the nucleus: when the nucleus possesses a weak quadrupole deformation (measured by the experimental ratio E_{4^+}/E_{2^+}) the agreement is worse than when the nucleus is well deformed. This pattern seems to indicate that the rotational formula, obtained under the assumption of a strongly deformed system [18, 6], is not valid when the nuclear deformation falls below certain limit that depends on mass number. Therefore, a sound calculation of transition strengths requires going beyond the rotational formula and therefore requires the introduction of angular momentum projected (AMP) wave functions.

2.3 Angular momentum projection

Angular momentum projection is the last step in our beyond mean field scheme but it will only be used here to compute transition strengths. The reason is that the calculation of transition strengths only requires the evaluation of one body operator overlaps which is a relatively inexpensive computational task. This is in contrast with the evaluation of two body operators, like in the evaluation

of hamiltonian overlaps, required to fully implement an angular momentum projected GCM where the f_σ amplitudes are determined by a projected Hill-Wheeler equation [19]. In the next section, we will project onto good angular momentum the GCM wave functions of Sect 2.2 without taking into account the effects of AM projection in the f_σ amplitudes. The projected wave functions will be used to compute norms and transition strengths.

In the present calculation an important simplification comes from the restriction to axially symmetric intrinsic states. Due to this symmetry the angular momentum projected state only involves $K = 0$ intrinsic states and is written as

$$|(\Psi_\sigma)_M^J\rangle = N_M^J P_{M0}^J |\Psi_\sigma\rangle \quad (4)$$

where N_M^J is a normalization constant and P_{MK}^J is the standard angular momentum operator

$$P_{MK}^J = \frac{2J+1}{8\pi^2} \int d\alpha d\beta d\gamma \mathcal{D}_{MK}^{J*}(\alpha, \beta, \gamma) \quad (5)$$

$$\times \exp\left(\frac{-i}{\hbar}\alpha J_z\right) \exp\left(\frac{-i}{\hbar}\beta J_y\right) \exp\left(\frac{-i}{\hbar}\gamma J_z\right)$$

To compute the transition strengths the calculation of the overlap of the electric multipole moment operator $Q_{\lambda\mu}$ (which is a tensor of rank λ) between projected states is required

$$\langle(\Psi_{\sigma'})_{M'}^{J'}|Q_{\lambda\mu}|(\Psi_\sigma)_M^J\rangle \quad (6)$$

For the E1 strengths the standard dipole operator, that takes into account center of mass effects, is considered instead. This is a quantity that can be evaluated using the magic of the Wigner-Eckart theorem and the final expression for the $B(E\lambda)$ only involves reduced matrix elements which are given in the present framework, restricted to axially symmetric intrinsic states, in terms of an integral in the rotation angle β – see [19] for a detailed derivation. Another characteristic of the calculation of even-even nuclei is that the intrinsic states are, by construction, eigenstates of the simplex operator $\mathcal{S} = \Pi R_y(\pi)$. As a consequence of this discrete symmetry, the projected states with angular momentum J must necessarily have the “natural parity” $\pi = (-1)^J$ and therefore only the 0^+ , 1^- , 2^+ , 3^- , etc are accessible.

A similar calculation aimed at the evaluation of E1 and E3 strengths was carried out in [5] but using instead of the GCM correlated wave functions the intrinsic wave functions obtained with the parity projected procedure of Sec 2.1. The differences between the results obtained by projecting the parity projected RVAP intrinsic states and the GCM ones were first analyzed in [20] where a few selected examples were considered in detail. The results discussed in this reference are summarized in Table 1 where an assorted set of nuclei regarding their ground state quadrupole deformation is discussed. Two facts stand out in this table: first the strong impact in the E3 transition strength of using AM projected wave functions when the nucleus is spherical as in the Pb case where we go from the 7.7 Weisskopf units (W.u) given by the rotational formula to 22 W.u. when AM projected wave functions are considered. The second fact is the relevance

Table 1. $B(E3, 3_1^- \rightarrow 0_1^+)$ transition strengths in W.u. for the different approaches considered. See text for notation. In all the cases, the suffix AMP represents Angular Momentum Projected calculations. The last column is the quadrupole deformation parameter β_2 for the ground state. Experimental data taken from [2] and [12].

	Exp	PP RVAP	PP AMP	GCM Q3	GCM AMP	β_2 (GS)
^{20}Ne	13	9.73	12.78	12.46	12.31	0.66
^{64}Zn	20 ± 3	10^{-4}	0.6	2.83	5.75	-0.21
^{158}Gd	12	9.43	10.29	13.73	12.64	0.34
^{208}Pb	34	7.07	23.06	7.67	21.93	0
^{224}Ra	42 ± 3	71.39	71.39	70.16	61.51	0.18

of using GCM wave functions instead of the parity RVAP for the calculation of those strengths as in several examples like ^{64}Zn , ^{158}Gd or even ^{224}Ra there are noticeable differences representing up to a 20% change. The reason is that in those nuclei, the quadrupole deformation shows relevant variations along the set of intrinsic wave functions $|\varphi(Q_3)\rangle$. Those variations can not be accounted for by just considering two intrinsic wave functions as in the RVAP case. An extreme example is ^{64}Zn that requires the explicit treatment of quadrupole and octupole degrees of freedom to obtain reasonable results. The theoretical predictions for the excitation energy of negative parity states obtained without AMP are given in the supplemental material of [3]. The corresponding AMP are much more computationally intensive and they are not available yet. Exploratory results reveal that the excitation energies do not differ much in the two cases, probably as a consequence of the scalar nature of the Hamiltonian, much simpler than the tensor one of the transition operators.

An interesting quantity is the probability of finding a state with angular momentum J and parity π in the intrinsic GCM wave function $|\Psi_\sigma\rangle$ and given by

$$\mathcal{P}^{J,\pi} = \left| \langle \Psi_\sigma | \hat{P}^{J,\pi} | \Psi_\sigma \rangle \right|^2 \quad (7)$$

where $\hat{P}^{J,\pi}$ is the standard angular momentum projector for axially symmetric configurations defined previously. In the present calculation, and due to the simplex symmetry of the intrinsic states, the only relevant probabilities are those for the states fulfilling the natural parity rule $\pi = (-1)^J$. For the other states not fulfilling this rule the probabilities are exactly zero. For well deformed intrinsic states the probability distribution as a function of J is expected to be broad with small amplitudes for a large range of J values [6]. On the other hand, when dealing with nearly spherical ground states the angular momentum $J = 3$ of the “octupole phonon” couples to the $J = 0$ of the ground state and therefore a probability distribution $\mathcal{P}^{J,\pi}$ strongly peaked at $J^\pi = 3^-$ is to be expected for the first negative parity state. This will be illustrated in the section devoted to the results below.

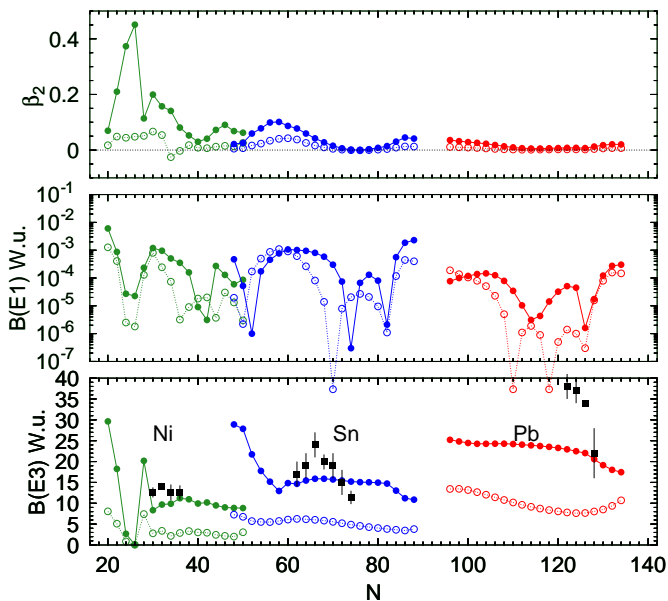


Fig. 1. Lower panel: the $B(E3, 3^- \rightarrow 0^+)$ transition strength (in W.u.) are plotted as a function of the neutron number of each isotope. Three isotopic chains corresponding to the Ni ($Z = 28$), Sn ($Z = 50$) and Pb ($Z = 82$) are plotted in green, blue and red, respectively. Open symbols connected with dotted lines represent the results obtained with the rotational formula whereas full symbols connected with full lines correspond to the calculation using angular momentum projected wave functions. Disconnected full squares with error bars correspond to the experimental results taken from the compilation of Ref [12]. Middle panel: $B(E1, 1^- \rightarrow 0^+)$ transition strength (in W.u.) are plotted as a function of the neutron number with the same color scheme as in the previous panel. Upper panel: the average quadrupole deformation parameter $\beta_{2\text{av}}$ for the 0^+ ground state (open symbols) and the lowest negative parity state (full symbols) are plotted as a function of neutron number.

3 Results

The purpose of this section is to present and discuss the results obtained in the one dimensional GCM framework, using the octupole moment Q_{30} as generating coordinate, and computing the transition strengths using the AMP wave functions, as described in Sect. 2. The nuclei considered in this study are those susceptible to show a significant failure of the rotational formula to compute transition strengths and include isotopic chains of nuclei with a proton number in the neighborhood of a magic number. We will consider isotopic chains of the elements Fe, Ni and Zn corresponding to the magic proton number 28, the chains of Cd, Sn, and Te for the magic number $Z=50$ and finally the chains of Hg, Pb, and Po corresponding to the magic proton number of 82.

In Fig 1 we present the main results of the present study for the semi-magic isotopes of Ni, Sn and Pb plotted as a function of neutron number. In the upper panel, the average quadrupole deformation parameter $\beta_{2\text{av}}$ for the intrinsic GCM ground state and the intrinsic first negative

parity excited state

$$\beta_{2\text{av}}(\sigma) = \sqrt{5/(16\pi)} 4\pi / (3r_0^2 A^{5/3}) \langle \Psi_\sigma | \hat{Q}_{20} | \Psi_\sigma \rangle \quad (8)$$

is plotted. In the Pb chain both quadrupole deformation parameters are very small, corresponding to spherical and negative parity excited states. In the Sn chain a similar behavior is observed for isotopes with large neutron number, close to $N = 82$. However for lower neutron numbers the negative parity excited state acquires a deformation of around 0.1 that goes back to spherical at $N = 50$. In the Ni case, the situation is a bit different, with spherical ground states near $N = 50$, but for the negative parity state there is some deformation even in this case. At lower neutron numbers, close to $N = 28$, the ground state is slightly deformed and the excited state is strongly deformed.

In the lower panel of Fig 1 the $B(E3, 3^- \rightarrow 0^+)$ transition strengths in W.u. are plotted for the three isotopic chains. Open symbols represent the results obtained from the intrinsic moments using the rotational formula. Full symbols are used to represent the results obtained with the AM projected states. In the Pb case, where both the 0^+ ground state and the first negative parity excited states are nearly spherical the projected results are in the whole isotopic chain a factor nearly three larger than the rotational formula results. The AM projected results are much closer to experimental data than the rotational formula results although there some noticeable differences still remain. In the Sn case, where both states are nearly spherical for most of the neutron number values, the enhancement due to projection is also strong and in the range of a factor three. There is an exception near $N=50$ where the negative parity excited state is also spherical and the enhancement factor grows up to nearly five. It would be interesting to measure the E3 strength in ^{100}Sn to assess this effect. The comparison with experimental data is very satisfactory when the AM projected wave functions are used, clearly indicating the necessity of using this kind of wave functions to compute transition strengths. Finally, in the Ni case, the trend is similar with strong enhancements of the E3 strengths when both the ground state and the negative parity one are near spherical and some accidents like in ^{54}Ni where the negative parity state is strongly deformed and the E3 strength shows a pronounced dip. As in the Sn and Pb cases, the agreement with experiment is very good when the AM projected wave functions are used in the calculation. It would be interesting to measure the E3 strength in both ^{54}Ni and ^{56}Ni to see if the predicted strong variation is observed experimentally as it would serve as an indicator of the strong quadrupole deformation of the excited state in ^{54}Ni .

Finally, in the middle panel of Fig 1 the E1 strengths are given as computed with both the rotational formula (open symbols) and the AM projected wave functions (full symbols). Clearly, the E1 transition is less collective than the corresponding E3 one, with transitions in the range of 10^{-3} W.u. As a consequence of the reduced collectivity, the E1 strengths depend more strongly on the details of the single particle structure around the Fermi level (like which orbital is filled) than in the deformation of the

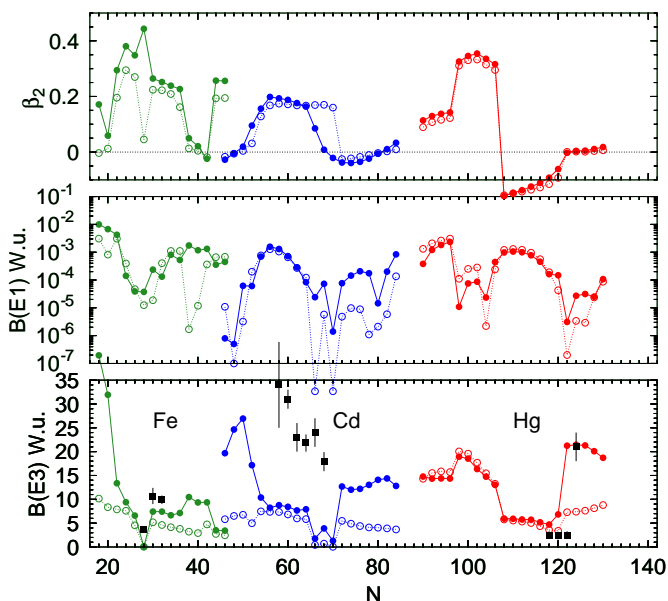


Fig. 2. Same as Fig 1 but for the Fe ($Z=26$), Cd ($Z=48$) and Hg ($Z=80$) isotopic chains.

ground and excited states. Therefore, no general trend is observed as in the E3 case and the E1 strengths are in some cases enhanced and in some cases reduced by factors as large as two orders of magnitude. Surprisingly, some dips observed in the evolution of the E1 with neutron number in the three isotopic chains when computed with the rotational formula are shifted when AM projected wave functions are used. This is the case, for instance in ^{200}Pb , ^{192}Pb or ^{12}Sn .

In Fig 2 the results corresponding to the isotopic chains with Z values two units less than magic and corresponding to Fe ($Z = 26$), Cd ($Z = 48$) and Hg ($Z = 80$) are shown. Contrary to the results of Fig 1 only those isotopes with neutron number close to a magic number remain spherical in both their ground and excited states. In those cases, the E3 strength computed with the AM projected wave functions are enhanced with respect to the rotational formula. As neutron number decreases there are transitions to oblate (Hg) and prolate (Cd and Fe) deformations. The AM projected E3 strength gets severely quenched and this offers a natural explanation of the sudden drop in E3 strength in the Hg isotopes. On the other hand, the comparison with experimental data in the Cd isotopes reveal a serious mismatch that can be attributed to the fact that, as we are not considering the quadrupole degree of freedom as dynamical variable, the effects of shape coexistence present in these isotopes (and observed in our mean field calculations with the Gogny force) is not accounted for in the present framework. In the Fe case, the sudden drop in E3 in the isotope ^{54}Fe is well reproduced and attributed to the different deformations of the ground state (spherical) and negative parity excited state (deformed with $\beta_2 = 0.45$). Regarding the E1 strengths, in the present case the differences between the strengths computed with the rotational formula and the ones with

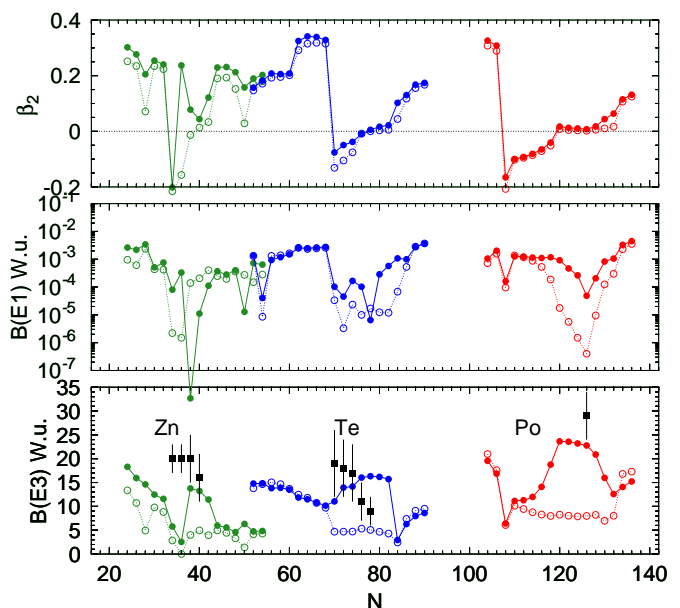


Fig. 3. Same as Fig 1 but for the Zn ($Z = 30$), Te ($Z = 52$) and Po ($Z = 84$) isotopic chains.

the AM projected wave functions are not so marked as in the previous case except in the Cd isotopes with $N > 62$ and the Fe isotopes around $N = 40$.

In Fig 3 the results corresponding to the isotopic chains with Z values two units more than magic and corresponding to Zn ($Z = 30$), Te ($Z = 52$) and Po ($Z = 84$) are shown. The results are very similar to the ones in Fig 2 and corresponding to Fe, Cd and Hg. However, there are some quantitative differences, as for instance, the broader interval of sphericity around magic neutron number in Po, the sudden oblate-prolate transition in Te or the singular case of ^{64}Zn with both states oblate. The latter case was studied in detail in [20] where the relevant role of the simultaneous treatment of quadrupole and octupole degrees of freedom as a consequence of shape coexistence was discussed. The same type of coupling could dramatically change the results obtained in ^{66}Zn and explaining the severe disagreement with experimental data. Apart from those two cases, the agreement with experiment is good and, as in previous cases, the use of AM projected wave functions proves to be of paramount relevance to obtain sound theoretical predictions. In the Po case, the E1 strengths computed with the AM projected wave functions are strongly enhanced with respect to the ones computed with the rotational formula for those isotopes which are spherical. This is also the case, although less prominent, for some heavy Te isotopes.

In Fig 4 the probability distribution $\mathcal{P}^{J,\pi}$ of Eq 7 corresponding to the first negative parity intrinsic GCM state is plotted as a function of the neutron number for all the nuclei considered in the present calculations and for J^π values 1^- , 3^- and 5^- . The results belong to two categories: for spherical nuclei, the probability of the 3^- is very large, typically exceeding 60% whereas for deformed nuclei, and irrespective of the sign of the β_2 parameter,

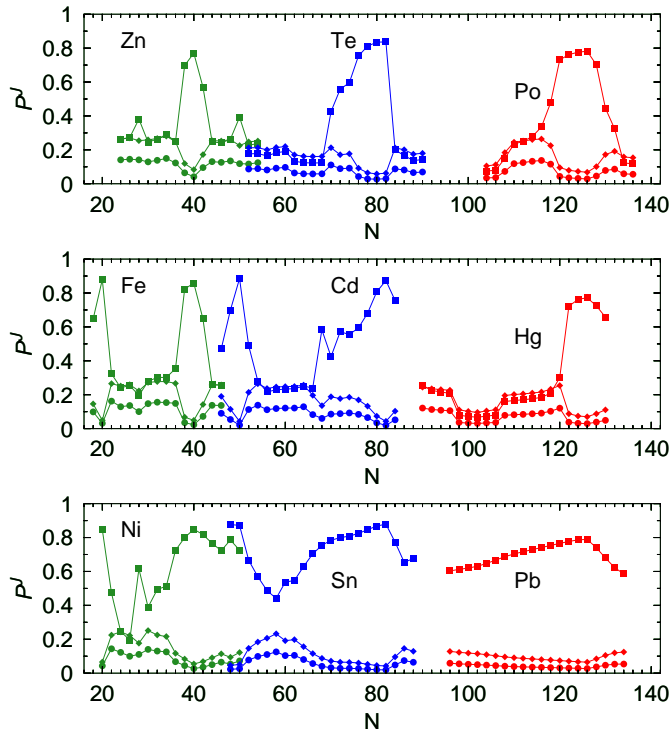


Fig. 4. Probability distributions $\mathcal{P}^{J,\pi}$ corresponding to $J^\pi = 1^-$ (bullets), $J^\pi = 3^-$ (filled boxes) and $J^\pi = 5^-$ (filled diamonds) for the lowest lying negative parity GCM state of each isotope are plotted as a function of the neutron number N of the isotope.

the probability distributions for all J^π values considered are small, of the order of 10%, and very similar for the different J values. In those cases where $\mathcal{P}^{3,-}$ is large we can talk about a vibrational state on top of an spherical ground state with a physical state in the laboratory system with quantum numbers 3^- . This is the case in most of the Ni and all the Sn and Pb isotopes considered. This feature explains very nicely the strong E3 strength observed, for instance, in ^{208}Pb (34 Wu). On the other hand, those states with small $\mathcal{P}^{J,\pi}$ values it is difficult to anticipate which would be the J^π of the lowest physical states and a full AM projected calculation is required to determine the $f_\sigma(Q_3)$ amplitudes of the GCM intrinsic states.

4 Conclusions

In this paper, the range of validity of the rotational formula commonly used to evaluate electromagnetic transition strengths is studied in the particular case of the E1 and E3 transitions between negative parity excited states and the ground state. It is shown that for those cases where one or the two quantum mechanic states involved is spherical or near spherical the rotational formula breaks down and the use of angular momentum projected wave functions is required for a sound evaluation of the required overlaps and transition strengths. Several isotopic chains with Z values near or at magic values have been analyzed

and the results compared to experimental data. The E3 transition strengths consistently show an enhancement of a factor (with respect to the rotational formula) between 2 to 4 when the AM projected wave functions are used in spherical or nearly spherical nuclei. The enhancement proves to be crucial to improve the agreement with experimental data. Clearly, such an enhancement is not observed in those nuclei with quadrupole deformed configurations where the rotational formula remains valid. On the other hand, the E1 transitions do not show a clear pattern as in the E3 case. This is due to the much less collective character of this transition. The present results indicate that for weakly deformed nuclear systems, the use of the rotational approximation to compute transition strengths is not justified and a more elaborated scheme including angular momentum projected wave functions is required. The rotational formula is often used the other way around, that is to extract β_3 values from transition strengths. Obviously this correspondence is wrong for spherical and near spherical nuclei and its consequences should be handled with care.

Acknowledgments

This work was supported by the Ministerio de Economía y Competitividad (MINECO) Spain, under Contracts Nos. FIS2012-34479, FPA2015-65929 and FIS2015-63770.

References

1. P.A. Butler, W. Nazarewicz, Rev. Mod. Phys. **68**, 349 (1996)
2. L.P. Gaffney, P.A. Butler, M. Scheck, A.B. Hayes, F. We- nander, M. Albers, B. Bastin, C. Bauer, A. Blazhev, S. Bonig et al., Nature **497**, 199 (2013)
3. L.M. Robledo, G.F. Bertsch, Phys. Rev. C **84**, 054302 (2011)
4. L.M. Robledo, Journal of Physics G: Nuclear and Particle Physics **42**, 055109 (2015)
5. L.M. Robledo, G.F. Bertsch, Phys. Rev. C **86**, 054306 (2012)
6. P. Ring, P. Schuck, *The nuclear many body problem* (Springer, Berlin, 1980)
7. J. Dechargé, D. Gogny, Phys. Rev. C **21**, 1568 (1980)
8. J.F. Berger, M. Girod, D. Gogny, Nucl. Phys. A **428**, 23 (1984)
9. S. Goriely, S. Hilaire, M. Girod, S. Péru, Phys. Rev. Lett. **102**, 242501 (2009)
10. F. Chappert, M. Girod, S. Hilaire, Phys. Lett. B **668**, 420 (2008)
11. L.M. Robledo, G.F. Bertsch, Phys. Rev. C **84**, 014312 (2011)
12. T. Kibédi, R. Spear, Atomic Data and Nuclear Data Tables **80**, 35 (2002)
13. R. Balian, E. Brezin, Il Nuovo Cimento B (1965-1970) **64**, 37 (1969)
14. L.M. Robledo, Physical Review C **50**, 2874 (1994)
15. L.M. Robledo, Phys. Rev. C **79**, 021302 (2009)

16. G.F. Bertsch, L.M. Robledo, *Phys. Rev. Lett.* **108**, 042505 (2012)
17. L.M. Robledo, *Journal of Physics G: Nuclear and Particle Physics* **37**, 064020 (2010)
18. A. Bohr, B. Mottelson, *Nuclear Structure*, Vol. II (Benjamin, New-York, 1975)
19. R. Rodriguez-Guzman, J.L. Egido, L.M. Robledo, *Nuclear Physics A* **709**, 201 (2002)
20. L.M. Robledo, *Improvements on the present theoretical understanding of octupole correlations*, in *European Physical Journal Web of Conferences* (2014), Vol. 66 of *European Physical Journal Web of Conferences*, p. 02091